An Algorithm for Diagnosis of the Three Kinds of Constitutional Jaundice

Shaker Ali, Zou Beiji, and Abbas Ali
School of Information Science and Engineering, Central South University, China

Abstract: *In this paper we have made an algorithm to diagnose the Constitutional Jaundice (Dubin-Johnson, Gilbert and Rotor syndrome) the algorithm is decomposed into two parts: 1) using Wavelet Transform to analyse the image; via Wavelet Transform we collected three features for each kind of disease 2) calculates the percentage of the gray scales (percentage of white and black colour) for each image via its histogram, it will collect two features for each kind of disease. In total there will be five values; these five values will be the inputs for the fuzzy logic that will decide the kind of disease based on these values. We made experiments for 55 cases mostly for children who suffered from different kinds of Constitutional Jaundice. Our algorithm yields more accurate results compared to the diagnosis by a doctor's eyes only.*

Keywords: *Medical diagnosis, Constitutional Jaundice, segmentation, Wavelet Transforms, and fuzzy logic.*

Received May 19, 2009; accepted August 3, 2009

1. Introduction

Constitutional Jaundice is rare disease which has little influence on either the well-being or longevity of the patient, it generally have a good prognosis. But the chronic hepatitis, especially the viral hepatitis, is a common disorder which is clinical, some patients presented few or lack symptom, liver function test also may be normal, however, they manifested by long continuous or fluctuating Jaundice. The Jaundice induced by Constitutional Jaundice often leads to a mistaken diagnosis and in confusion [8].

We need to find an accurate and high precision algorithm to diagnose the Constitutional Jaundice. In medical diagnosis there are several specific requirements that the system must meet, as in our paper we need to cut only the infected part from the image, we then need to use the Wavelet Transform (WT) to analyse the image to get some features, the final result will be decided by the fuzzy logic.

Image segmentation is an integral part of image processing applications like medical images analysis and photo editing. A wide range of computational vision algorithms can also benefit from the existence of reliable and efficient image segmentation technique. For instance, intermediate-level vision problems such as shape from silhouette, shape from stereo and object tracking could make use of reliable segmentation of the object of interest from the rest of the scene. Higher-level problems such as recognition and image indexing can also make use of segmentation results in matching [1, 17].

After segmenting an image, we have to extract some features that allow fuzzy logic to easily detect features of the disease by analysing the image using WT.

Wavelets were recently developed mathematical tool for capturing dynamic characteristics of non-stationary signal using short-data window. The potential benefits of applying WT for analysis of transient fault signals in power systems have been recognized in the recent years and Rosa *et al.* have reported an overview of application of wavelets in power systems [11].

The WT plays a substantial role in multi-resolution techniques, particularly in the last decade it was used in several digital image processing applications [10]. WT plays an important role in the image processing analysis, cheaply in texture recognition of data, for its fine result when using multi-resolution modelling [2]. After analysing the images, we need to pick up many features, which are the key to exploring the different kind of diseases via fuzzy logic.

The fuzzy modelling system is developed to model a system with some descriptive fuzzy logic rules that are designed to deal with complex, ill-defined and unconstrained problems. The two main purposes of fuzzy logic are; (i) to make an accurate and quick procedure to approach the desired result; (ii) to build a general and flexible mechanism which is applicable in solving various fields of modelling problems [6].

Accuracy is very important in classifiers used for medical applications. A high percentage of false negatives in screening systems increase the risk of real patients not receiving the attention they need, while a high false alarm rate causes unwarranted worries and increases the load on medical resources. In the quest

for higher classification accuracies and improved diagnosis, the concept of committee (ensemble) classifiers has been adopted in medicine; e.g., [9, 13]. Section 2 explains the 3 types of the Constitutional Jaundice. Section 3 describes our algorithm, the experiments are explained in section 4, and at last, conclusion is drawn in section 5.

2. Constitutional Jaundice

Constitutional Jaundice is the result of a highly specific function in one of the discrete steps in the hepatic pathway for translocation of bilirubin (red-yellow pigment in urine, blood and bile) from blood to bile. According to present knowledge, three main kinds of Constitutional Jaundice can be distinguished [5, 7, 8].

2.1. Dubin-Johnson Syndrome

Dubin-Johnson (D-J) syndrome is a benign autosomal recessive condition in which biliary secretion of bilirubin pigment is defective. The defect is due to the absence of the canalicular protein MRP2 located on chromosomes 10q 24, which is responsible for the transport of biliary glucuronides and related organic anions into bile [5].

Electronic microscopic observation of the D-J syndrome cases revealed abundant pigment granules in the cytoplasm of hepatocytes. The pigment granule was mainly composed of dense granular material; however the lighter elements of lipid nature were only detectable in places shown in Figure 1(a) [7, 8].

2.2. Gilbert's Syndrome

It is so far the most frequent of all Constitutional Jaundice (inherited hyperbilirubinemias). It presents at the time of puberty and its prevalence in young persons amounts to 5 - 8%. Total hyperbilirubinemia usually does not exceed 80 μmol/l and direct bilirubin is less than 20%. Hyperbilirubinemia conditions leads to pigment accumulation. The pigment granules contains only a minor amount of the proteinic granular-filamentous component, which surrounds in frame-like manner the bulk of the pigment body, formed by lipid globules. This is shown in Figure 1(b) [7, 8].

2.3. Rotor's Syndrome

It is in many respects similar to the Dubin-Johnson syndrome. In clinical, D-J and Rotor syndromes all have conjugated hyperbilirubinemias. The ultra structural features of the pigment granules found in the Rotor syndrome contain approximately equal parts of proteinic granules filamentous and lipid globules, as shown in Figure 1(c) [7, 8].

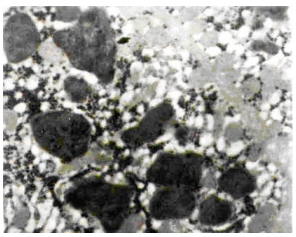

a. Dubin-Johnson syndrome.

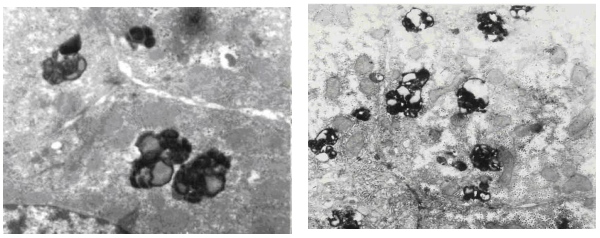

b. Gilbert's syndrome. c. The Rotor's syndrome.

Figure 1. The syndromes.

3. The Algorithm

The algorithm is designed to diagnose the three types of constitution Jaundice (Gilbert, Rotor and Dubin-Johnson syndrome) the aim of our work is to develop an algorithm based on image processing technology for diseases diagnose to replace the classical diagnosis which depends on the doctor's eyes only. We also aim at improving microscopy by removing its most serious limitation: reliance on the performance of a human operator for diagnostic accuracy [14].

The algorithm consists of two parts; the two parts are having four common steps: image acquisition, pre-processing, segmentation and classification. The first part has two extra steps; image analysis and feature extraction. The second one is to compute the percentage of the gradation gray scales for each kind of disease by using appropriate threshold depending on the histogram, as shown in Figure 2.

3.1. Image Acquisition

Images are acquired using an electronic microscope with 1,000X magnification, but the images from the electronic microscope are negative, so we need to obtain the normal ones, images are captured in the JPEG format, with maximum resolution size 544×665 pixels, which were later resized to 512×512 pixels.

3.2. Pre-Processing

The aim of pre-processing is to enhance the images and remove unwanted effects; image enhancement refers to any process by which the visual quality of an image is improved. Because there could be significant variations in the acquired images due to varying lighting conditions, camera types, and so on, there are no set procedures to be adopted in image enhancement. Generally speaking, enhancement techniques are ad hoc in nature [13].

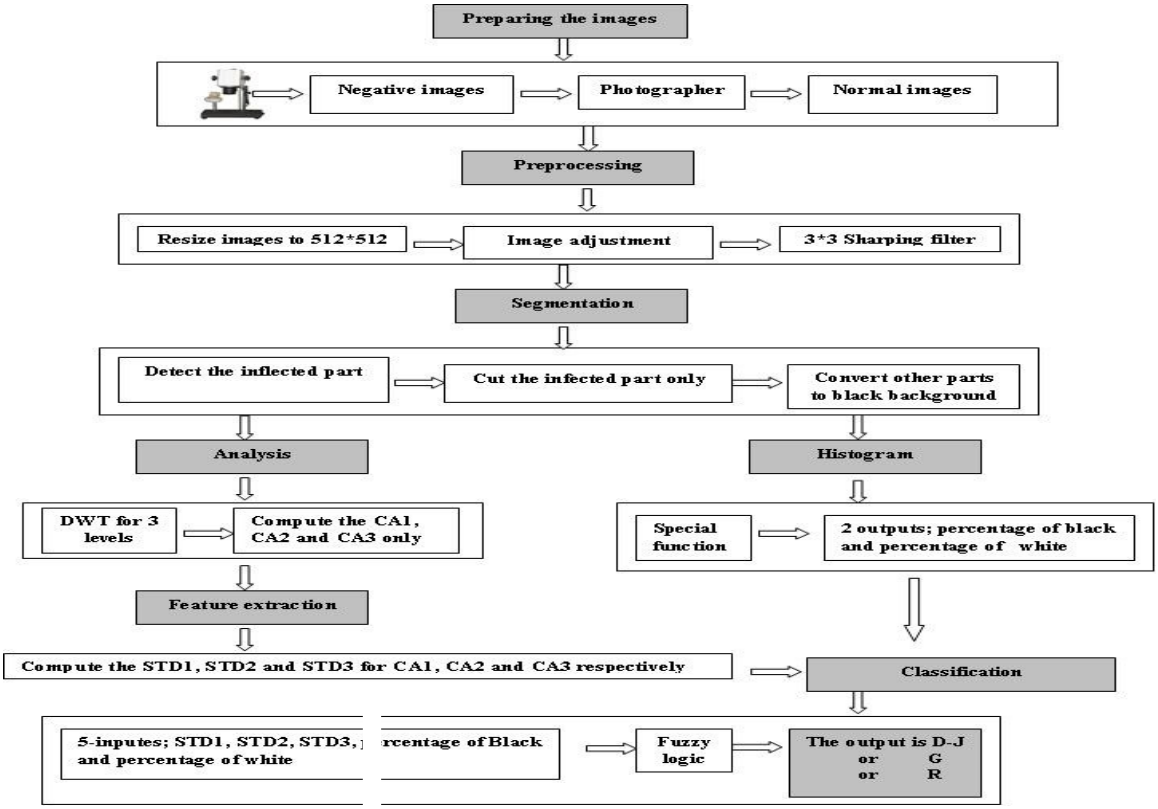

Figure 2. The steps of our algorithm.

Image adjustment which removes the unwanted part of the image that came from some noises (converted from negative to normal ones) is the first step. High contrast for the image is needed in our work.

In some case even when the dynamic range of an image is within that of the display device, the image may still have low contrast. This may be due to poor lighting conditions under which the image was captured or due to a smaller dynamic range of the capturing device. In such cases a simple rescaling of the pixel intensities might be adequate to improve the visibility. This involves a piecewise linear transformation of the input pixel intensities. Such a transformation can be expressed by the following equation [13].

$$y = \begin{cases} ax, 0 \le x < x_1 \\ b(x - x_1) + y_{x1}, x_1 \le x < x_2 \\ c(x + x_2) + y_{x2}, x_2 \le x < B \end{cases} \quad (1)$$

where *a*, *b*, and *c* are appropriate constants, which are the slopes in the respective regions, and B is the maximum intensity value. The intent here is to enlarge low values and reduce high values of the pixel intensities while keeping the intermediate values approximately intact.

The second step is applying 3 x 3 sharpening filters to the image which is sharpened by subtracting a blurred version of the image from itself, as shown in Figure 3.

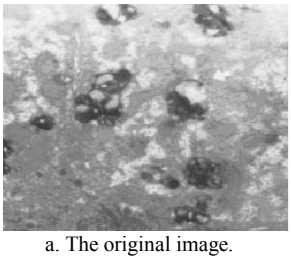

a. The original image.

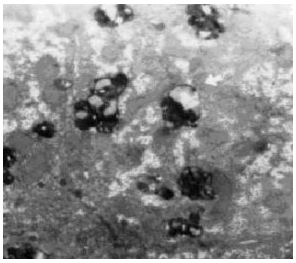

b. After image adjustment.

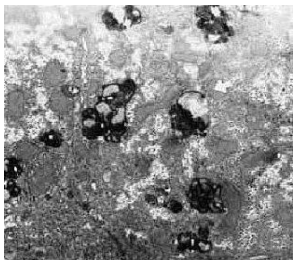

c. After sharpening filter.

Figure 3. Image adjutant and filtering.

3.3. Segmentation (Using Grow Cut Method)

Segmentation is the stage where a significant commitment is made during automated analysis by delineating structures of interest and discriminating them from background tissue [13]. Some algorithms useful in segmentation give good results, for our experiments we found that the grow cut method is useful for our work, and it is based on the following idea:

The bacteria start to spread (grow) from the seed pixels and try to occupy the entire image. That is why

they called the method 'Grow Cut'. The rules of bacterial growth and competition are obvious, at each discrete time step; each cell tries to 'attack' its neighbours. The attack force is defined by the attacker cell's strength, and the distance between attacker's and defender's feature vectors. Using this segmentation method, one can easily cut the infected part and converts the background to black as shown in Figure 4. If the attack force is greater than defender's strength, then the defending cell is 'conquered' and its label and strength is changed [16].

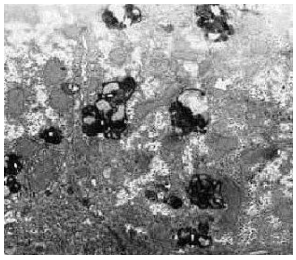

a. Source image.

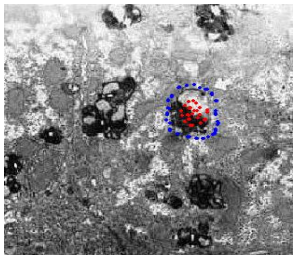

b. User-specified seeds.

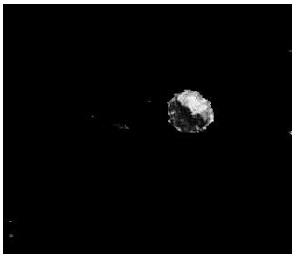

c. Segmentation results.

Figure 4. Segmentation method.

3.4. Image Analysis

In order to extract the most important features, we need to try the best way for analysis, so we tried with Discrete Wavelet Transform (DWT), it yields more accurate results. WT are widely applied in many fields for solving various problems. The Fourier Transform of a signal contains the frequency contents of the signal over the analysis window and, as such, lacks any time domain localization information. In order to achieve time localization information it is necessary for the time domain to be short, therefore compromising frequency localization. On the contrary to achieve frequency localization requires large time analysis window and time localization is compromised. There in lies the dilemma sometimes referred to as the "uncertainty principle". The Continuous Wavelet Transform (CWT) of a signal, *x(t),* is the integral of the signal multiplied by scaled and shifted versions of a wavelet function and is defined as in equation 2 [15].

$$CWT\ (a,b) = \int_{-\infty}^{\infty} x(t) \frac{1}{\sqrt{|a|}} \psi\left(\frac{t-b}{a}\right) dt \quad (2)$$

where *a* and *b* are so called the scaling (reciprocal of frequency) and time localization or shifting parameters, respectively. Calculating wavelet coefficients at every possible scale is computationally a very expensive task. Instead, if the scales and shifts are selected based on powers of two, so-called dyadic scales and positions, then the wavelet analysis will be much more efficient. Such analysis is obtained from the DWT which is defined as,

$$DWT\ (j,k) = \frac{1}{\sqrt{|2^j|}} \int_{-\infty}^{\infty} x(t) \psi\left(\frac{t-2^j k}{2^j}\right) dt \quad (3)$$

where a and b are replaced by *2j* and *k2j*, respectively. Mallat developed an efficient way for implementing this scheme by passing the signal through a series of Low-Pass (LP) and High-Pass (HP) filter pairs named as quadrature mirror filters [1].

In the first step of the DWT, the signal is simultaneously passed through a LP and HP filters with the cut-off frequency being one fourth of the sampling frequency. The outputs from the low and high pass filters are referred to as Approximation (A1) and Detail (D1) coefficients of the first level, respectively. The output signals having half the frequency bandwidth of the original signal can be down sampled by two according to Nyquist rule. The same procedure can be repeated for the first level approximation and the detail coefficients to get the second level coefficients. At each step of this decomposition process, the frequency resolution is doubled through filtering and the time resolution is halved through down sampling.

Figure 5 shows the third level wavelet decomposition of a signal [7]. These convolution functions are filters; one half of the output is produced by the LP filter in equation 4.

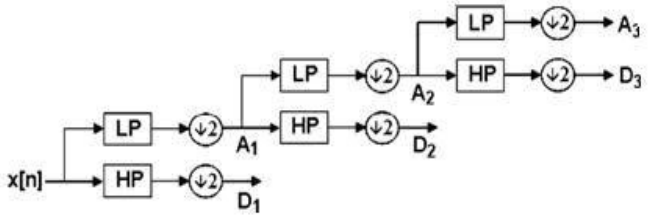

Figure 5. Third level wavelet decomposition of a signal.

$$L_i = \frac{1}{2} \sum_{j=1}^{N} c_{j+1-2i} \times f_j \quad (4)$$

while the other half is produced by HP filter as in equation 5:

$$H_i = \frac{1}{2} \sum_{j=1}^{N} (-1) c_{2i-j} \times f_j \quad (5)$$

where *i=1,2,.....N/2, N* is the input of row size, *C's*: are the coefficients, *L* and *H* are the output functions.

In many situations, the LP output contains most of the "information content" of the input row. The HP output contains the differences between the true input

and the value of the reconstructed input, if it is to be reconstructed from only the information given in the LP (detailed) output.

The output of the LP filter consists of the average of every two sample, and the output of the HP filter consists of the difference of two samples [3].

3.5. Feature Extraction

The purpose of feature extraction is to collect new variables from the matrix of the image that concentrates information to separate classes. Most systems perform feature extraction as a pre-processing step, in obtaining global image features like colour histogram or descriptors like shape and texture. Texture features have been modelled on the marginal distribution of wavelet coefficients using generalized Gaussian distributions [3].

After wavelet decomposition of the image that contains only the infected part use, we can extract some important features that come from the using of Bior6.8 and Sym4 by using mean and standard deviation. The mean is implemented as in equation 6 [2].

$$mean = \frac{1}{RS}\sum_{r=0}^{R-1}\sum_{s=0}^{S-1} f(r,s) \tag{6}$$

The STandard Deviation (STD) is implemented as in equation 7:

$$STD = \sqrt{\frac{\sum_{r=0}^{R-1}\sum_{s=0}^{S-1}(f(r,s)-mean)^2}{R*S}} \tag{7}$$

where *f(r,s)* is the value of the pixel in this position. The most important features will be the key for fuzzy logic to make the final decision about the type of the disease; more details will be in the experiment section.

3.6. Classification Using (Fuzzy Modelling Systems Structure)

For Multi-Inputs Single Output (MISO) fuzzy modelling systems, the description of fuzzy rules can be illustrated as follows: *R(i): if X is xj* then *Y* is *yi, i ={1,2,...,m}* where *X= (x1, x2 ..., xn)* are linguistic variables, represents the i^{th} rule, *xj* are fuzzy sets of the input vector(*x*) in the premise part and *yi* is a real number in the consequent part. *m* is the number of total rules, the definition of the fuzzy set is described by the membership function shown in equation 8 [14].

$$ME_i = \exp(-(\frac{(x_i - a_{i1})^2}{b^2_{i1}} + ... + \frac{(x_n - a_{in})^2}{b^2_{in}})) \tag{8}$$

This can be considered that there is a hyper-ellipsoid in an *n*-dimensional space. where $(a_{i1},a_{i2},...,a_{in})$ is the center of the hyper-ellipsoid and (b_{ij}) is the length of the j^{th} principal axis of the hyper-ellipsoid.

The simple weighted average defuzzier is taken to convert fuzzy domain into real value. If the firing strength of the premise part in i^{th} rule is deserved, the actual output *Y* of the fuzzy system can be calculated as in equation 9.

$$Y = \frac{\sum_{i=1}^{m} ME_i(x) \bullet y_i}{\sum_{i=1}^{m} ME_i(x)} \tag{9}$$

According to the above description, the contour of the membership function *MEi(x)* which defined by parameters $\{a_{i1}, b_{i1}, a_{i2}, b_{i2},..., a_{in}, b_{in}\}$ and the real value of consequent parameter *yi* determines a fuzzy system. Thus, different parameters set $\{a_{i1}, a_{i2}, ... , a_{in}, b_{i1}, b_{i2}, ... b_{in}, y_i, 1\_ i\_m\}$ decide different fuzzy system with different initial setting. If there are *m* fuzzy rules to construct, the *m x (2n +1)* parameters in this parameter set $\{ a_{i1}, a_{i2}, ... , a_{in}, b_{i1}, b_{i2}, ... b_{in}, y_i, 1\_ i\_m \}$ need to be determined for designing such fuzzy systems. There are *m* fuzzy rules with *n* input variables at the start, so we must discover *m* hyper-ellipsoids in an *n* dimensional space [2, 16].

There are many types of Fuzzy Neural Network (FNN), for the forward multi-layer fuzzy neural network, the typical ones are Mamdani model, Sugeno model and Tsukamoto model f. The simple and widely used Sugeno model is applied in this paper. For simplicity, we assume that there are three rules in the fuzzy reasoning system of Sugeno model:

R1: If STD1 is low, STD2 is low, STD3 is low, PB is low and PW is low, then f1 is D-J.
R2: If STD1 is medium, STD2 is medium, STD3 is medium, PB is medium and PW is medium, then f2 is G.
R3: If STD1 is high, STD2 is high, STD3 is high, PB is high and PW is high, then f3 is R.

where *STD1, STD2, STD3, PB* (percentage of black) and *PW* (percentage of white) are the input variable; low, middle and high are fuzzy subsets of *STD1, STD2, STD3*, *PB* and PW; *fi* is the conclusion of the fuzzy rule and the function of input variable *STD1, STD2, STD3*, *PB* and PW; D-J, *G* and *R* are Dubin-Johnson, Gilbert and Rotor, respectively. The operation of FNN is Gradient descent method. The aim is the minimization of the error function $E = 1/2\ (d-y)^2$ where, *y* is the output of the fuzzy logic, d is the expected output of the i^{th} sample. The weight w_{ij} is trained by the learning rules illustrtrated in equations 10 and 11. [4].

$$w_{ij}(t+1) = w_{ij}(t) - \eta\frac{\partial E}{\partial w_{ij}} \alpha\Delta w_{ij}(t) \tag{10}$$

$$\Delta w_{ij}(t) = w_{ij}(t) - w_{ij}(t-1), \tag{11}$$

where η is the learning velocity, $\alpha(0 < \alpha < 1)$ is the gradient.

4. Experiments

We collected 55 cases mostly for children that suffered from different kinds of the Constitutional Jaundice. These cases collected from the Xiang Ya Hospital in Changsha, Hunan, China from (1990-2008). The conducted experiments have been very beneficial for medical treatment and perm solving many problems in an easier manner. The following steps are followed to implement our algorithm:

1. *Read the image; enhance it by raising the contrast of the image by using image adjustment method.*
2. *Call "grow cut" function.*
   New image= segmentation mask old image*
3. *Convert the background to black and keep the infected part only*
4. *Calculate CA1,CA2 and CA3 (the approximately parts of WT for three levels respectively)*
5. *Calculate std1, std2 and std3 for CA1, CA2 and CA3 respectively.*
6. *From step 2 we remove the back ground and keep only the part that had contain the information of the disease to find the PB and white(PW) in each kind of disease by using special function.*
7. *Five features (std1, std2, std3, PB and PW) will be the inputs of the fuzzy logic.*

Our results are divided into four steps shown in the following sections.

Step 1: image enhancement method.

There types of enhancement method (image adjustment, logarithmic transformation and histogram equalization) are used. Experiments reveal that image adjustment plays the most important role in obtained the result; as shown in Table 1, in this table we took two images of (D-J), they are tackled as a sample to check the best enhancement method. Table 1 shows that when we use the image adjustment the difference of the STD between the two samples is from (1-3), but when others technique has been used, the difference is from (6-60).

Step 2: feature extraction.

Many types like (entropy, mean, moment and standard deviation) have been used but at the end of our experiments we found that the best ones are STD and mean; as shown in Table 1, the mean had some interference so we resorted to using STD as feature for diagnosis only, which gives us good result as shown in Figure 6.

Table 1. Image adjustment is the best enhancement method.

Enhancement Method	FE	D-J1	D-J2	Dif.
Image Adjustment	**std1**	35	36	1
	std2	64	65	1
	std3	115	112	3
	mean1	139	102	37
	mean2	278	205	73
	mean3	557	413	144
Logarithmic Transformation	**std1**	31	44	13
	std2	59	77	18
	std3	106	123	17
	mean1	135	107	28
	mean2	270	214	56
	mean3	540	428	112
Histogram Equalization	**std1**	52	45	7
	std2	103	81	22
	std3	197	137	60
	mean1	151	106	45
	mean2	303	213	90
	mean3	611	428	183

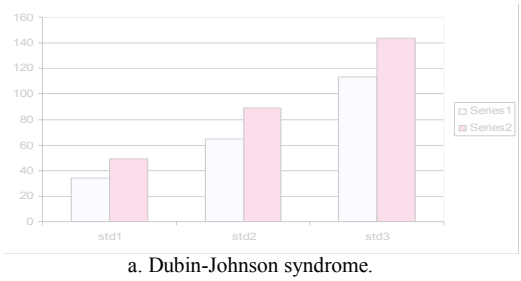

a. Dubin-Johnson syndrome.

b. Gilbert syndrome.

c. Rotor syndrome.

Figure 6. STD values of the three diseases kinds.

We collected the values of STDs of the (D-J, G and R) in Table 2. (4-values for each kind of disease), then, the range values (minimum and maximum) for each kind have been evaluated as shown in Table 3. These values will be as three inputs for the fuzzy logic.

Table 2. STD, PB, and WP values.

		Std1	Std2	Std3	Black Percentage	White Percentage
Diseases Type	D-J1	38	72	132	99.0188	0.9122
	D-J2	39	76	137	81.4246	18.6453
	D-J3	37	70	129	86.3316	13.8448
	D-J4	40	78	140	72.7859	27.2586
	G1	96	191	376	0.1429	99.9524
	G2	98	192	367	29.7256	703506
	G3	90	188	370	28.9345	71.1632
	G4	99	201	380	9.1431	90.9518
	R1	167	328	627	46.9404	53.2146
	R2	170	330	630	48.004	51.911
	R3	172	333	634	51.999	48.009
	R4	166	320	642	43.656	56.355

Table 3. STD, PB, and PW values range.

	Std1	Std2	Std3	Percentage of Back	Percentage of White
D-J	35-43	60-80	120-150	70-100	0-30
G	85-105	180-220	360-385	0-35	65-100
R	160-180	315-140	620-650	41-52	46-58

Step 3: wavelet families.

In this paper, all types of families (db, Haar, symb, coif, bior,…*etc.,*) are used. The experimental results show that Symb4 and Bior6.8 are the best ones. They gave us great results and have near values for those images in the same group (has the same disease) and far values for those images in different group (disease). From the segmentation step we need the infected part only, after removing the background to determine the percentage of black and white gray scale in each kind, the histograms are used to extract some details, depending on these details, the percentage of the white and black for each picture can be calculated. A close look to the histogram, it is easy to see the different between the three kinds of disease in as shown in Figure 7. the percentage of black and white for each kind is shown in Table 2, these values can be used to be the second key of the fuzzy logic, so that we use these value to collect the range values of the (PB and PW) percentage of the black and white respectively as illustrated in Table 3, these will be two inputs for fuzzy logic add to three input from STDs, in totally there will be five inputs, form these values the fuzzy will be easing decide the kind of the disease.

In this paper, two groups have been used. The first one contained 50% from the images that we used as source (desired), the second group contained 50% from the images as a test images. After applying testing the algorithm the result from fuzzy logic has been very accuracies with (95%-100%) as shown in Table 4.

Table 4. The fuzzy logic results.

Disease Name	No. of Cases	Fuzzy Accuracy
Rotor	11	95%
D-J	32	100%
Gilbert	12	98%

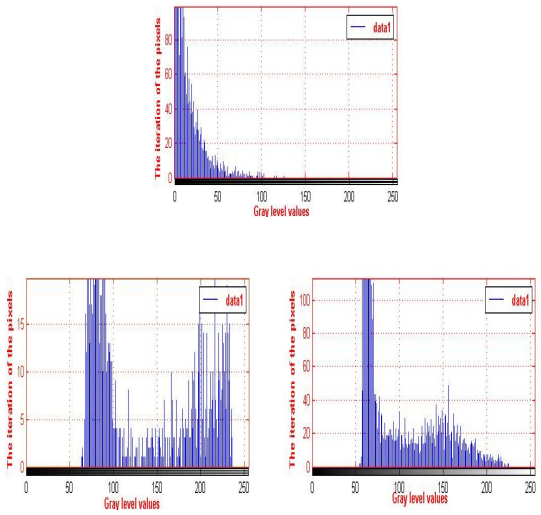

Figure 7. Histograms of Dubin-Johnson, Gilbart, Rotor, respectively.

5. Conclusions

In this paper, we tried many methods for enhancement as wavelet families and feature extraction. We found that: for enhancement method; image adjustment was the best enhancement method for our algorithm, for wavelet families; Bior6.8 or Symb4, are the best for analysis and good results for our experiments by using the approximate parts of WT for three levels only and for feature extraction; STD was the best one for our algorithm and without using the mean because the worst case happens when the mean is used.

Acknowledgements

This research is funded by: National Natural Science Foundation of China (Project No. 60970098), Hunan Provincial Natural Science Foundation of China (Project No. 07JJ3125), Major Program of National Natural Science Foundation of China (Project No. 90715043), Changing Scholars and Innovative Research Team in University (Project No. IRT0661) and National Natural Science Foundation of China (Project No. 60803024).

References

[1] Ali S. and Zou B., "Analysis and Classification of Remote Sensing by Using Wavelet Transform and Neural Network," *in Proceedings of International Conference on Computer Science and Software Engineering*, pp. 963-966, 2008.

[2] Al Mahtab M., Fazal K., Rahman S., and Muhammad A., "Dubin Johnson Syndrome with Systemic Lupus Erythematosus: A Case Report," *Computer Journal of Hepatobiliary Pancreat Dis International*, vol. 5, no. 4, pp. 159-163, 2006.

[3] Bankman I., *Handbook of Medical Imaging Processing and Analysis*, Academic Press, 2000.

[4] Feng H., "A Self-Tuning Fuzzy Control System Design," *in Proceedings of 9th IFSA World Congress and 20th NAFIPS International Conference*, Vancouver, pp. 209-214, 2001.

[5] Feng H., "Hybrid Stages Particle Swarm Optimization Learning Fuzzy Modeling Systems Design," *Computer Journal of Tamkang Journal of Science and Engineering*, vol. 9, no. 2, pp. 167-176, 2006.

[6] Gopinath P. and Reddy N., "Toward Intelligent Web Monitoring: Performance of Committee Neural Networks vs. Single Neural Network," *in Proceedings of the IEEE International Conference on Information Technology Applications in Biomedicine*, pp. 179-182, 2000.

[7] Jayabharata R. and Mohanta D., "A Wavelet-Fuzzy Combined Approach for Classification and Location of Transmission Line Faults," *in Proceedings of Elsevier, Electrical Power and Energy Systems*, pp. 29 669-678, 2007.

[8] Jianguo Z. and Tieniu T., "Brief of Invariant Texture Analysis Method," *Computer Journal of Pattern Recognition*, vol. 35, no. 2, pp. 735-747, 2002.

[9] Johannessen J., *Electron Microscopy in Human Medicine*, McGraw-Hill, 1979.

[10] Ocak H., "Automatic Detection of Epileptic Seizures in EEG Using Discrete Wavelet Transform and Approximate Entropy," *in Proceedings of Elsevier Expert Systems with Applications*, pp. 2027-2036, 2009.

[11] Park J., Oh M., and Han S., "Fish Disease Diagnosis System Based on Image Processing of Pathogens' Microscopic Images," *in Proceedings of Frontiers in the Convergence of Bioscience and Information Technologies*, pp. 878-883, 2007.

[12] Peng L., Li S., and Zhang S., "Differential Diagnosis in Electron Microscope of Conststutional Jaundice and Chronic Hepatitis," Rcenet Development of Electon Microscopy, pp. 175-177, 1990.

[13] Peters B., Pfurtscheller G., and Flyvbjerg H., "Automatic Differentiation of Multichannel EEG Signals," *in Proceedings of IEEE Transaction Biomedical Engineering*, pp. 111-116, 2001.

[14] Thyagarajan K., *Digital Image Processing with Application to Digital Cinema*, Elsevier Press, 2006.

[15] Unser M., "Texture Classification and Segmentation Using Wavelet Frames," *Computer Journal of IEEE Transaction on Image Processing*, vol. 4, no. 11, pp. 1549-1560, 1995.

[16] Vezhnevets V. and Konouchine V., "GrowCut: Interactive Multi-Label N-D Image Segmentation by Cellular Automata," *in Proceedings of Graphicon*, pp. 150-156, 2005.

[17] Wilson R., "Multiresolution Image Modeling," *Computer Journal of Electronic and communication Journal*, vol. 1, no. 2 , pp. 90-96, 1997.

Shaker Ali is a PhD candidate at the School of Information Science and Engineering, Central South University, People's Republic of China. Interest area of research is digital image processing, medical image processing, data security.

Zou Beiji is the vice dean and head of School of Information Science and Engineering, Central South University, People's Republic of China. Interest area of research is digital image processing, computer graphics, multi-media technology, and software engineering.

Abbas Ali is MSc student at the School of Information Science and Engineering, Central South University, People's Republic of China. Interest area of research is digital image processing, computer graphics, and semantic web.